Microgrid Planning Including Renewables Considering Optimum Compressed Air Energy Storage Capacity Determination Using HANN-MDA Method

Mohammad Mirshams[1], Seyed Amin Saeed[2*], Tahere Daemi[3], Zohreh Beheshtipour[4]

Department of Electrical Engineering, Yazd Branch, Islamic Azad University, Yazd, Iran. amin.saied@iau.ac.ir

Abstract

Microgrids, with their ability to integrate renewable energy sources, play a crucial role in achieving sustainable and resilient energy systems. Effective planning and optimization of microgrids, particularly considering the inclusion of compressed air energy storage (CAES) systems, are essential for maximizing their benefits. This study proposes a novel approach, the Hybrid Artificial Neural Network-Modified Dragonfly Algorithm (HANN-MDA), for determining the optimum capacity of CAES in microgrid planning. The HANN-MDA method combines the learning capabilities of artificial neural networks with the optimization power of the modified dragonfly algorithm. The proposed method aims to minimize the overall cost of microgrid operation while considering the integration of renewable energy sources and the storage capabilities of CAES. Simulation results demonstrate the effectiveness of the HANN-MDA method in accurately determining the optimal CAES capacity, leading to improved microgrid performance and cost savings. The findings highlight the importance of considering CAES in microgrid planning and the potential of the HANN-MDA method for achieving efficient and economically viable microgrid designs.

Keywords: Microgrids, Compressed Air Energy Storage, Hybrid Artificial Neural Network, Modified Dragonfly Algorithm
Article history: Received 2024/01/18; Revised 2024/03/02; Accepted 2024/03/10, Article Type: Research paper

1. Introduction

The increasing integration of renewable energy sources into power systems has spurred the need for advanced planning strategies to enhance grid resilience, reliability, and sustainability. Microgrids (MGs), as localized and self-sufficient energy systems, have emerged as a promising solution to address these challenges [1]. This research focuses on the intricate domain of microgrid planning, emphasizing the critical role of Compressed Air Energy Storage (CAES) systems in mitigating uncertainties associated with renewable energy sources, ultimately aiming for cost minimization. In recent years, the global energy landscape has witnessed a transformative shift towards cleaner and more sustainable alternatives as shown in Figure (1). The escalating concerns about climate change, coupled with advancements in renewable energy technologies, have accelerated the adoption of solar, wind, and other clean energy sources. However, the inherent intermittency and variability of renewables pose significant challenges to the stability and reliability of power grids. MGs which characterized by their decentralized nature and ability to operate independently or in conjunction with the main grid, offer a viable solution to integrate renewables seamlessly [2].

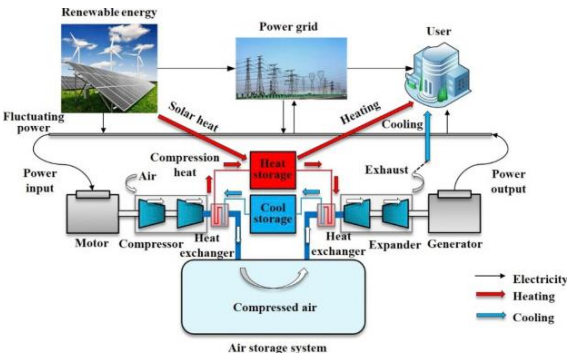

Fig. 1. a typical microgrid equipped with CAES [2]

Microgrid planning involves the optimal allocation of resources, considering both the demand and supply sides. The integration of renewable energy sources, such as solar and wind, adds complexity due to their fluctuating nature [3]. Accurate forecasting and management of these uncertainties are paramount for ensuring a stable and efficient microgrid operation. This research aims to delve into the nuances of microgrid planning, focusing on effective strategies to accommodate renewable energy sources and mitigate their inherent variability. CAES systems have emerged as a promising technology to address the intermittency challenges associated with renewables [4]. By storing excess energy during periods of abundance and releasing it during high demand, CAES enhances grid stability and reliability. However, determining the optimum capacity of CAES is a complex task, especially when considering uncertainties associated with renewable energy generation. This research aims to develop a comprehensive framework for microgrid planning that incorporates the optimal determination of CAES capacity, taking into account the uncertainties inherent in renewable energy sources. Microgrid planning is a multidimensional optimization problem that requires careful consideration of various factors, including energy demand, generation capacity, storage capabilities, and economic constraints. The dynamic nature of renewable energy sources adds an additional layer of complexity to this optimization process. Traditional approaches may fall short in providing effective solutions that balance these diverse and dynamic parameters. This research seeks to address this gap by proposing an advanced optimization model that integrates the uncertainties associated with renewables, with a specific focus on determining the optimum capacity of CAES [5-7]. Optimum scheduling in an economic MG involves determining the optimal operation of the MG to minimize its operating costs while meeting the energy demand of its local consumers. One key factor in optimizing the operation of a MG is the determination of the optimum capacity of its energy storage systems. It could be determined based on several factors such as the energy demand profile of the local consumers, the availability and cost of the distributed generation sources and the price of electricity in the upstream network [8]. The energy storage system capacity needs to be large enough to store excess energy generated from renewable sources during times when the demand for electricity is low and supply energy during times when the demand for electricity is high. To determine the optimum capacity of energy storage systems, an optimization model can be developed that considers various factors such as the energy demand profile, the availability and cost of the distributed generation sources, and the price of electricity in the upstream network. The objective of the optimization model is to minimize the operating costs of the MG while meeting the energy demand of its local consumers. Once the optimum capacity of energy storage systems is determined, the MG can be operated to minimize its operating costs while meeting the energy demand of its local consumers [9].

A) Literature Review and Research Gap

This paper introduces a novel optimization framework that focuses on scheduling Distributed Energy Resources (DERs) within MGs, with particular emphasis on determining the optimal energy storage capacity. The proposed methodology takes into account economic factors, technical considerations, and the dynamic behavior of DERs to achieve improved economic efficiency and reliability in MG operation [10]. In a related study, the performance of various optimization algorithms, including genetic algorithm, particle swarm optimization, and dynamic programming, is compared for scheduling DERs in MGs. The results highlight the effectiveness and computational efficiency of these different techniques. Another review paper provides an overview of economic dispatch strategies in MG operation. The authors discuss different objective functions, dispatch strategies, and their impact on optimizing economic performance, considering the integration of DERs and Energy Storage Systems (ESS) [11]. Furthermore, a methodology is presented in a separate paper for determining the optimum energy storage capacity in MG systems. This approach considers economic factors, technical considerations, and the dynamic behavior of DERs to determine the most suitable energy storage capacity [12]. A different study investigates the integration of renewable energy sources and energy storage systems in MGs. The authors discuss the benefits, challenges, and optimization strategies for scheduling DERs while considering the determination of energy storage capacity [13]. A review paper explores various methodologies for sizing energy storage systems in MGs, comparing deterministic and probabilistic approaches. The economic and technical considerations involved in energy storage sizing are highlighted [14]. In addition, a paper proposes a stochastic economic dispatch model for MGs that takes into account the uncertainty of DERs. The authors analyze the effect of uncertainty on MG operation and demonstrate improved economic performance [15]. Another study presents a multi-objective optimization approach for economic dispatch of DERs in MGs,

considering cost minimization, emission reduction, and reliability enhancement as conflicting objectives [16]. To tackle optimal scheduling and energy storage capacity determination, a hybrid algorithm combining particle swarm optimization and artificial neural networks is proposed in a paper. This approach demonstrates improved convergence and accuracy [17]. Load forecasting techniques and their application in MG scheduling are reviewed in another paper. Accurate load forecasting is crucial for optimal scheduling while considering energy storage capacity determination [18]. A robust scheduling strategy is proposed in a paper for DERs in MGs, considering probabilistic energy storage sizing. The approach accounts for uncertainties in DERs and optimizes MG operation under various scenarios [19]. Another study focuses on energy storage sizing for enhancing MG resilience. An optimization framework is proposed that considers the capacity and performance of energy storage systems to ensure reliable and resilient MG operation [20]. A real-time scheduling approach for DERs in economic MGs is presented in a paper. The authors consider the dynamic behavior of DERs and optimize their dispatch in response to changing grid conditions [21]. Optimal power flow modeling for MGs, with a focus on determining the optimum energy storage capacity, is proposed in another paper. The authors demonstrate improved economic efficiency and reliable operation of MGs using this model [22]. The integration of demand response management with MG scheduling, considering energy storage capacity determination, is investigated in a study. The authors analyze the impact of demand response on economic performance and grid stability [23]. A comprehensive framework for optimal scheduling of DERs with energy storage in economic MGs is proposed in a paper. Various factors such as cost, reliability, and environmental impact are considered to optimize MG operation [24]. The effect of energy storage capacity on MG stability and resilience is analyzed in a study. The authors examine the relationship between storage capacity, DERs, and grid stability under different operating conditions [25]. An optimal allocation method for energy storage systems in MGs is addressed in a paper. The authors propose a method that considers the location, capacity, and cost of energy storage to optimize MG performance [26]. The impact of DER and ESS integration on MG operation costs is analyzed in a study. The authors quantify the economic benefits and cost savings achieved through optimized scheduling and energy storage capacity determination [27]. Finally, authors in [28] paper investigates the enhancement of renewable energy utilization in economic MGs through optimal scheduling. Scheduling strategies are proposed to maximize the utilization of renewable energy sources while considering energy storage capacity determination.

While the existing literature provides valuable insights into microgrid planning, renewable energy integration, and the role of CAES, there is a noticeable gap in research specifically addressing the dynamic uncertainties associated with renewables in the context of CAES integration within microgrids. The need for a comprehensive optimization model that considers these uncertainties and determines the optimal CAES capacity is evident, pointing to the motivation for the current research.

B) Research Objectives

This research holds significant implications for the advancement of microgrid planning strategies in the context of increasing renewable energy integration. The developed optimization model, incorporating CAES capacity determination and addressing uncertainties, is expected to contribute to more resilient and cost-effective microgrid designs. By optimizing the deployment of CAES, the research aims to enhance the overall efficiency of microgrids and accelerate their adoption as a sustainable solution for decentralized energy generation. Therefore, the primary objectives of this research are as follows:

- Develop a comprehensive understanding of microgrid planning and the challenges posed by the integration of renewable energy sources.
- Investigate the role of CAES in mitigating uncertainties associated with renewables and enhancing microgrid stability.
- Propose an optimization model that considers the dynamic nature of renewable energy generation and determines the optimum capacity of CAES for cost minimization.
- Evaluate the proposed model through simulations and case studies to demonstrate its effectiveness in real-world microgrid scenarios.

C) Research Structure

The remainder of this research will be organized as follows: Section 2 represents the methodology, so that as an in-depth exploration of the proposed optimization model, detailing the incorporation of renewable uncertainties and the determination of optimal CAES capacity are investigated. A brief review on optimization algorithm is represented in Section 3. The results and discussion are presented in Section 4 as presentation and analysis of simulation results, demonstrating the effectiveness of the proposed model in diverse microgrid scenarios. The discussions are represented in Section 5. Finally, a

summary of key findings, implications, and avenues for future research in the field of microgrid planning and renewable energy integration are expressed in Section 6 as the conclusion.

2. Methodology

Optimizing a microgrid with diverse energy resources, including renewable sources, microturbines, and a CAES system, involves a complex framework aimed at achieving multiple objectives. Microgrids represent a modern approach to decentralized and sustainable energy systems. The integration of renewable energy sources, such as wind turbines (W) and solar photovoltaics (PV), alongside conventional generators like microturbines (M) and innovative storage solutions like CAES, offers a robust and resilient energy infrastructure. The primary goal is to formulate an optimization framework that minimizes the total planning costs while ensuring reliable and environmentally conscious microgrid operation.

The framework involves several decision variables, each influencing the microgrid's operation. These include power outputs of generators $P_g(t)$, renewable power outputs ($P_w(t)$, $P_s(t)$, CAES compression and discharge powers $P_{\text{caes\_c}}(t)$, $P_{\text{caes\_d}}(t)$, CAES energy level $E_{\text{caes}}(t)$, power not served $P_{\text{ens}}(t)$, excess power $P_{\text{ex}}(t)$, and emissions of pollutants $E_p(t)$. The overarching objective is to minimize the total planning costs (J). This cost includes the generation costs of wind (C_w), solar (C_s), and microturbine (C_m) sources, the cost of energy not served (C_{ens}), the cost of excess generation (C_{ex}), and penalty costs associated with pollutant emissions $\left(CP(p)\right)$. The objective function encapsulates economic, environmental, and reliability considerations.

$$\mathrm{J} = \sum_{t\in T}\left(\begin{matrix} C_w \times P_w(t) + C_s \times P_s(t) + C_m \times P_m(t) \\ + C_{\text{ens}}(t) + C_{\text{ex}}(t) + \sum_{p\in P} C\,P(p) \times E_p(t) \end{matrix}\right) \qquad (1)$$

A) Power Balance Constraints

The power balance equation ensures that the total electric power generated from various sources, accounting for CAES processes and considering excess or deficit power, matches the electric load demand at each time period. Here is the refined version of the power balance equation:

$$\begin{aligned} P_g(t) + P_w(t) + P_s(t) + P_{caes\_d}(t) - P_{caes\_c}(t) \\ + P_{ex}(t) - P_{ens}(t) \\ = D(t)\ \forall\, t \in T \end{aligned} \qquad (2)$$

This equation expresses the equilibrium between the sum of power outputs from generators ($P_g(t)$), wind turbines ($P_w(t)$), solar PV ($P_s(t)$), and CAES discharge ($P_{\text{caes\_d}}(t)$), minus the CAES compression ($P_{\text{caes\_c}}(t)$), plus excess power ($P_{\text{ex}}(t)$) and minus the power not served ($P_{\text{ens}}(t)$), which equals the electric load demand ($D(t)$) at each time period ($\forall\, t \in T$). This equation forms the foundation for maintaining a stable and balanced operation of the microgrid, ensuring that the total power supplied meets the demand at all times.

B) Renewable Power Output Constraints

These constraints limit the power output of wind turbines and solar PV, accounting for uncertainties $U_w(t)$ and $U_s(t)$. The constraints ensure that the generated renewable power does not exceed the specified maximum values, considering variations due to uncertainties, and contribute to maintaining grid stability.

$$P_w(t) \le P_{w\max}(t) \times \left(1 + U_w(t)\right) \forall t \in T \qquad (3)$$

$$P_s(t) \le P_{s\max}(t) \times \left(1 + U_s(t)\right) \forall t \in T \qquad (4)$$

To account for uncertainties in renewable energy sources, the power outputs of wind turbines and solar PV are modified by uncertainty factors $U_w(t)$ and $U_s(t)$. These uncertainties reflect the variations in wind and solar power generation, ensuring a more realistic representation of the renewable energy inputs in the optimization framework.

C) CAES Energy Limits

These constraints define the allowable range for the energy stored in the CAES system. It prevents overcharging or complete depletion, ensuring the CAES system operates within its capacity limits and contributes effectively to grid stability.

$$0 \le E_{\text{caes}}(t) \le E_{\text{caesmax}}\ \forall t \in T \qquad (5)$$

D) Generator Output Limits

These constraints impose upper bounds on the power output of each generator (wind turbines, solar PV, microturbines). They prevent excessive generation that could lead to operational challenges and contribute to the overall control of the microgrid.

$$0 \le P_g(t) \le P_{g\max}\ \forall g \in G,\ \forall t \in T \qquad (6)$$

E) CAES Compression/Discharge Limits

These constraints regulate the power flow during CAES compression and discharge processes, ensuring they operate within the specified efficiency limits. They play a crucial role in optimizing the CAES system's performance and efficiency.

$$0 \le P_{\text{caes\_c}}(t) \le \frac{E_{\text{caes}}(t)}{\text{eff\_c}}\ \forall t \in T \qquad (7)$$

$$0 \le P_{\text{caes\_d}}(t) \le E_{\text{caes}}(t) \times \text{eff\_d}\ \forall t \in T \quad (8)$$

F) Emission Calculations

These equations quantify the emissions of pollutants (CO_2, SO_2, NO_x) based on the power output of each generator and their respective emission rates. It helps in assessing the environmental impact of the microgrid operation and guides decision-making towards cleaner energy sources.

$$E_p(t) = \sum_{g \in G} E_g(p) \times P_g(t)\ \forall p \in P,\ \forall t \in T \quad (9)$$

G) Non-negativity Constraints

These constraints enforce that all decision variables, including power outputs, energy levels, and emissions, remain non-negative. It reflects the physical constraints of the system, preventing unrealistic or negative values.

$$P_g(t), P_w(t), P_s(t), P_{\text{caes\_c}}(t), P_{\text{caes\_d}}(t), P_{\text{ens}}(t), P_{\text{ex}}(t), E_p \ge 0\ \forall g \in G,\ \forall t \in T,\ \forall p \in P \quad (10)$$

H) CAES Compression Energy

This equation calculates the energy consumed during CAES compression. It considers the compression power, efficiency, and time interval, providing insights into the energy requirements for storing compressed air in the CAES system.

$$E_{\text{caes\_c}}(t) = P_{\text{caes\_c}}(t) \times \text{eff\_c} \times \Delta t\ \forall t \in T \quad (11)$$

I) CAES Expansion Energy

Similar to the compression energy equation, this calculates the energy released during CAES expansion. It is a key component in understanding the energy dynamics of the CAES system during discharge.

$$E_{\text{caes\_d}}(t) = P_{\text{caes\_d}}(t) \times \text{eff\_d} \times \Delta t\ \forall t \in T \quad (12)$$

J) CAES Compression Exergy

This equation computes the exergy (availability to do work) associated with the compressed air during CAES compression. It's a thermodynamic measure reflecting the quality of the stored energy in the CAES system.

$$\text{exergy}_{\text{caes\_c}}(t) = \frac{P_{\text{caes\_c}}(t) \times \text{eff\_c} \times \Delta t}{T_0}\ \forall t \in T \quad (13)$$

K) CAES Expansion Exergy

Similar to compression exergy, this equation calculates the exergy associated with the expanded air during CAES discharge. It provides insights into the thermodynamic efficiency of the CAES process.

$$\text{exergy}_{\text{caes\_d}}(t) = \frac{P_{\text{caes\_d}}(t) \times \text{eff\_d} \times \Delta t}{T_0}\ \forall t \in T \quad (14)$$

L) CAES Compression Exergy Efficiency

This equation defines the exergy efficiency during CAES compression. It quantifies how effectively the compression process converts input energy into exergy, offering a measure of the system's thermodynamic performance.

$$\text{eff\_exergy\_caes\_c}(t) = \frac{\text{exergy}_{\text{caes\_c}}(t)}{QLHV}\ \forall t \in T \quad (15)$$

M) CAES Expansion Exergy Efficiency

Parallel to compression exergy efficiency, this equation characterizes the exergy efficiency during CAES expansion. It evaluates the effectiveness of the CAES system in converting stored energy into useful work.

$$\text{eff\_exergy\_caes\_d}(t) = \frac{\text{exergy}_{\text{caes\_d}}(t)}{QLHV}\ \forall t \in T \quad (16)$$

N) CAES Compression Exit Temperature

This equation calculates the exit temperature of air after compression in the CAES system. It considers the compression power, efficiency, and thermodynamic properties, providing insights into the thermal aspects of the compression process.

$$T_{\text{caes\_c\_exit}}(t) = T_0 \times \left(1 - \left(\frac{P_{\text{caes\_c}}(t)}{P_0}\right)^{\frac{n-1}{n}}\right)\ \forall t \in T \quad (17)$$

O) CAES Expansion Exit Temperature

Similar to compression exit temperature, this equation determines the exit temperature of air during CAES expansion. It offers valuable information on the thermal conditions at the end of the expansion process.

$$T_{\text{caes\_d\_exit}}(t) = T_0 \times \left(1 - \left(\frac{P_{\text{caes\_d}}(t)}{P_0}\right)^{\frac{n-1}{n}}\right)\ \forall t \in T \quad (18)$$

P) CAES Polytropic Index Limits

These constraints restrict the polytropic index within specified bounds. The polytropic index influences the thermodynamic behavior of the compressed air, and these limits ensure it stays within a reasonable range for stable operation.

$$n_{\min} \le n \le n_{\max} \quad (19)$$

Q) CAES Inventory Energy Limit

This equation ensures the conservation of energy in the CAES inventory, preventing energy

imbalances between compression and discharge processes. It contributes to the overall energy accountability within the CAES system.

$$E_{\text{caes\_inventory}}(t) = E_{\text{caes\_c}}(t) - E_{\text{caes\_d}}(t)\ \forall t \in T \quad (20)$$

R) CAES Compression Air Costs

This equation computes the cost associated with compressing air in the CAES system, considering the cost of air and operational parameters. It helps in evaluating the economic implications of the compression process.

$$C_{\text{caes\_air}}(t) = Ca \times \frac{P_{\text{caes\_c}}(t) \times \Delta t}{\text{eff\_c}}\ \forall t \in T \quad (21)$$

S) CAES Thermal Efficiency

This equation defines the thermal efficiency of the CAES system during discharge. It quantifies the ratio of useful work output to the energy input, providing a measure of the system's overall energy conversion efficiency.

$$\text{eff\_thermal\_caes}(t) = \frac{P_{\text{caes\_d}}(t)}{P_{\text{caes\_c}}(t)}\ \forall t \in T \quad (22)$$

T) Cost of Energy Not Served

This equation calculates the cost associated with the energy not served to meet the demand. It represents the economic consequences of insufficient power generation and guides decision-making to minimize such costs.

$$C_{\text{ens}}(t) = C_{\text{ens}} \times P_{\text{ens}}(t)\ \forall t \in T \quad (23)$$

U) Cost of Excess Generation

Similar to energy not served, this equation computes the cost associated with excess generation beyond the demand. It reflects the economic impact of overgeneration and aids in optimizing the microgrid operation economically.

$$C_{\text{ex}}(t) = C_{\text{ex}} \times P_{\text{ex}}(t)\ \forall t \in T \quad (24)$$

V) Generator Emission Penalties

These constraints limit the product of pollutant emissions and penalty costs for each generator. They provide an upper bound on the economic impact of emissions from the generators, facilitating environmentally conscious decision-making.

$$CP(p) \times E_p(t) \le M_{\text{emission}}\ \forall p \in P,\ \forall t \in T \quad (25)$$

These constraints ensure that the total economic impact of emissions from each generator, weighted by the penalty costs ($CP(p)$), remains within acceptable bounds (M_{emission}). It promotes a balance between economic considerations and environmental sustainability, aligning with the overarching goal of minimizing total planning costs.

W) Maximum Renewable Power

These constraints restrict the power output of wind turbines and solar PV to their respective maximum values, accounting for uncertainties $U_w(t)$ and $U_s(t)$. They play a crucial role in preventing excessive renewable energy generation, which could lead to operational challenges and contribute to grid instability.

$$P_w(t) \le P_{w\max}(t) \times \left(1 + U_w(t)\right) \forall t \in T \quad (26)$$

$$P_s(t) \le P_{s\max}(t) \times \left(1 + U_s(t)\right) \forall t \in T \quad (27)$$

X) Microturbine Limits

These constraints ensure that the power output of microturbines remains within specified minimum and maximum values. They contribute to the overall control of the microgrid and prevent operational challenges associated with microturbine power.

$$P_m(t) \ge P_{m\min}\ \forall t \in T \quad (28)$$

$$P_m(t) \le P_{m\max}\ \forall t \in T \quad (29)$$

These constraints on microturbine power output serve as important operational limits, preventing underutilization or overloading of microturbine assets in the microgrid.

Y) Demand Response

Demand response (DR) plays a pivotal role in influencing and enhancing the proposed microgrid planning framework. The integration of demand response mechanisms introduces a dynamic element that significantly impacts the optimization of microgrid operations, renewable energy integration, and the determination of CAES capacity. Here are the key effects:

DR introduces flexibility by allowing the microgrid to dynamically respond to changes in energy demand. This enhances the adaptability of the microgrid planning framework, enabling real-time adjustments to optimize energy generation, consumption, and storage. By incorporating demand response, the microgrid gains the ability to actively manage energy consumption during peak demand periods. This results in improved grid stability and reliability, reducing the risk of overloads and enhancing overall system resilience.

DR facilitates better utilization of available resources by aligning energy consumption with periods of high renewable energy generation. This optimization ensures that energy storage systems, including CAES, are utilized efficiently, minimizing waste and reducing operational costs. DR mechanisms contribute to economic benefits by

allowing the microgrid to participate in demand-side management programs. This enables the microgrid to capitalize on favorable pricing conditions, reduce peak demand charges, and potentially generate revenue through demand response participation.

The effect of DR on microgrid planning is particularly pronounced when integrating renewable energy sources. DR enables the alignment of energy consumption with periods of high renewable generation, maximizing the utilization of clean energy and reducing dependence on non-renewable sources. DR allows for dynamic load balancing, enabling the microgrid to optimize the distribution of energy based on real-time demand fluctuations. This ensures efficient utilization of generation and storage resources, contributing to overall energy efficiency.

The inclusion of demand response in the microgrid planning framework helps mitigate grid congestion during peak demand periods. By encouraging load-shifting and load reduction strategies, DR reduces stress on the grid and minimizes the risk of system failures. DR enhances the microgrid's ability to withstand disruptions by actively managing energy demand. This improved energy resilience is crucial in the face of uncertainties, contributing to the overall reliability and robustness of the microgrid.

DR can influence the operation of CAES systems by aligning energy consumption with periods of low demand or high renewable energy availability. This ensures that CAES operates optimally, supporting grid stability and minimizing the need for additional energy sources. The effect of demand response extends to the integration of advanced technologies, such as smart grids and IoT devices. These technologies enhance the responsiveness of demand-side management, providing real-time data for more accurate decision-making within the microgrid planning framework.

In general, the incorporation of demand response in the microgrid planning framework brings about a multitude of positive effects, ranging from improved grid stability and economic benefits to optimized resource utilization and enhanced resilience. This dynamic interaction strengthens the overall sustainability and efficiency of microgrid operations in the face of evolving energy landscapes, as can be formulates like the following:

$$P_l(t) \le Demand_{\mathrm{tl}}, \qquad \forall(\mathrm{t} \in \mathrm{T})\ and\ (l \in L) \tag{30}$$

$$P_l(t) \ge (1 - x_{\mathrm{tl}}^{DR}) \cdot Demand_{\mathrm{tl}}, \quad \forall(\mathrm{t} \in \mathrm{T})\ and\ (l \in L) \tag{31}$$

$$x_{\mathrm{tl}}^{DR} \in \{0,1\}, \qquad \forall(\mathrm{t} \in \mathrm{T})\ and\ (l \in L) \tag{32}$$

Totally, the optimization framework for a microgrid with renewable energy sources, microturbines, and a compressed air energy storage system is a sophisticated mathematical model. It balances economic, environmental, and operational considerations to achieve the overarching goal of minimizing total planning costs. The inclusion of decision variables such as power outputs, energy levels, and emissions, along with associated constraints, captures the complexity of microgrid dynamics. The objective function encapsulates the economic aspect by considering generation costs, costs of energy not served, costs of excess generation, and penalty costs for pollutant emissions. The power balance equation ensures that energy supply matches demand at each time period, forming the basis for stable microgrid operation. Renewable power output constraints and generator output limits prevent excessive generation and contribute to overall system stability. The incorporation of CAES introduces a storage mechanism that enhances the microgrid's capability to balance intermittent renewable generation with varying demand. The thermodynamic aspects, including CAES energy limits, compression and discharge processes, exergy efficiency, and exit temperatures, provide insights into the energy dynamics and performance of the storage system. Incorporating uncertainties in renewable energy sources adds a layer of realism to the model, acknowledging the inherent variability in wind and solar power generation. This enhances the robustness of the optimization framework, allowing for more accurate predictions of the microgrid's performance under real-world conditions.

3. Optimization Algorithm

An Artificial Neural Network (ANN) consists of interconnected nodes, or artificial neurons, organized in layers. The input layer receives the input data, which is then passed through hidden layers to the output layer. Each neuron performs a weighted sum of its inputs, applies an activation function, and passes the result to the next layer. The weights and biases of the neurons determine the behavior and performance of the network [28-30]. Let's denote:

x: Input vector of size n ($x = [x1, x2, \ldots, xn]$)

y: Output vector of size m ($y = [y1, y2, \ldots, ym]$)

W: Weight matrix ($n \times h$) connecting the input layer to the hidden layer

B: Bias matrix ($1 \times h$) for the hidden layer

V: Weight matrix ($h \times m$) connecting the hidden layer to the output layer

C: Bias matrix ($1 \times m$) for the output layer

f: Activation function (e.g., sigmoid, $ReLU$)

The output of the hidden layer can be calculated as:

$$H = f(x * W + B) \quad (33)$$

And the output of the network can be calculated as:

$$O = f(H * V + C) \quad (34)$$

The goal is to find the optimal values for the weight matrices W and V, as well as the bias matrices B and C, by minimizing a loss function that measures the discrepancy between the predicted output O and the actual output y.

The Modified Dragonfly Algorithm is (MDA) the optimization algorithm inspired by the swarming behavior of dragonflies. It consists of a population of solutions (dragonflies) and iteratively updates their positions to find the optimal solution. Let's denote:

X: Position matrix $(n \times h + h \times m)$ representing the weights and biases of the neural network

L: Fitness matrix $(1 \times h + 1 \times m)$ representing the performance of each solution

X_b: Global best position

L_b: Global best fitness

X_n: Neighboring position

L_n: Neighboring fitness

α: Attraction coefficient

β: Randomization parameter

ϵ: Randomization factor

γ: Step size

The steps of the Modified Dragonfly Algorithm can be summarized as follows:

Step 1: Initialize the population of dragonflies with random positions X and evaluate their fitness L.

Step 2: Update the global best position and fitness:

If $L > L_b$, set $L_b = L$ and $X_b = X$.

Step 3: Update the position of each dragonfly:

Generate a random number ϵ between 0 and 1.

For each dragonfly:

Calculate the distance between the current position X and the global best position Xb.

Update the position:

$$X = X + \alpha * (X_b - X) + \beta * (X_n - X) + \epsilon * \gamma * (rand - 0.5) \quad (35)$$

Where $rand$ is a random number between 0 and 1.

Evaluate the fitness L of the updated position.

Step 4: Repeat Steps 2 and 3 until a termination criterion is met (e.g., maximum number of iterations).

By integrating the MDA optimization process into the training of the neural network, the HANN-MDA approach aims to improve the convergence speed and accuracy of the network. To implement a HANN-MDA, these general steps would be addressed:

- Initialize the population of dragonflies with random positions, representing the weights and biases of the ANN.
- Evaluate the fitness of each dragonfly by training the ANN using the corresponding position and measuring its performance on a training dataset. The fitness value could be based on a performance metric such as accuracy, error rate, or loss function.
- Update the global best position and fitness by comparing the fitness values of the dragonflies.
- Update the position of each dragonfly based on the MDA update equations, taking into account the global best position, neighboring positions, and randomization parameters.
- Evaluate the fitness of the updated positions.
- Repeat steps 3 to 5 for a certain number of iterations or until a termination criterion are met (e.g., convergence).
- After the optimization process, use the global best position (representing the optimal weights and biases) to obtain the final trained ANN model.

4. Simulation Results

The study assumes that the MG incorporates decentralized power generation sources like micro turbines and fuel cells. These sources are spread across the MG and installed at various locations. Figure (1) displays the complete load curve of the MG for a specific day, showcasing the power requirements throughout the day. This data offers valuable information about energy consumption patterns and facilitates an understanding of the MG's operational behavior. Additionally, Figure (2) presents the fluctuations in the time of use (ToU) cost associated with using the grid during different hours of the day.

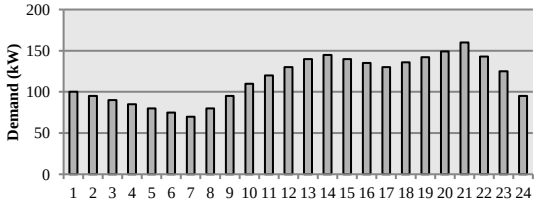

Fig. 2. Daily load profile for under studied MG

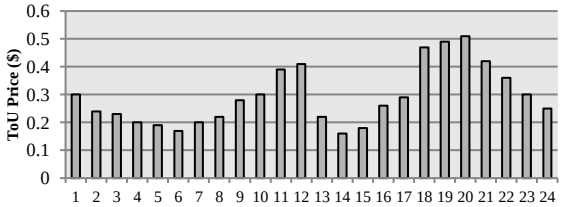

Fig. 3. ToU cost for under studied MG

Table 1 illustrates the minimum and maximum utilization boundaries for both the distributed production resources and the entire system. This table provides a comprehensive overview of the effective utilization limits for these resources. The minimum exploitation limits ensure that the resources are sufficiently utilized to meet the system's energy demands. Conversely, the maximum exploitation limits indicate the threshold beyond which the resources should not be pushed to avoid operational issues or inefficiencies. This crucial information ensures the optimization of resource utilization and the smooth functioning of the system. Stakeholders can make informed decisions about the deployment and operation of these resources by understanding and adhering to these exploitation limits. This ultimately leads to improved system performance and reliability. Table 1 also highlights that during a financial day, the exchange of electrical energy between the grid and the MG should not exceed a threshold of 200 kilowatts. This limitation ensures that the energy flow between these entities remains within an acceptable range, preventing imbalances or strain on the system. By adhering to this restriction, stable and reliable operation is maintained. Additionally, Table 1 provides detailed information on the costs associated with utilizing the distributed production resources, presented in dollars per kilowatt-hour (kWh). This data offers insights into the financial implications of leveraging these resources in the MG. Stakeholders can analyze the cost information to make informed decisions about the most economically viable utilization of these resources. This knowledge enables them to optimize resource allocation, prioritize cost-effective options, and improve financial management and overall efficiency.

The first case study assumes that the MG operates in island mode without any energy storage within the system. In contrast, the second scenario assumes the MG also operates in island mode but incorporates the installation of storage devices. Both cases have a project lifespan of 18 years. In island mode, the MG functions independently of the main grid. However, the absence of energy storage in the first case limits the MG's ability to effectively manage fluctuations in energy generation and demand. On the other hand, the second case, with storage devices, provides improved flexibility and resilience. It allows the MG to store excess energy during low-demand periods and release it during peak-demand periods. In all the mentioned scenarios, the project duration is set to 18 years. This timeframe ensures a comprehensive evaluation of the project's feasibility, cost-effectiveness, and long-term sustainability. By considering a consistent project lifespan, stakeholders can assess the economic viability and overall performance of the MG system over an extended period. This facilitates informed decision-making and strategic planning.

A) Islanding mode without ESS

The findings for the unit production arrangement during the day and night, based on the provided load profile, are displayed in Figure (4). The production quantities of the units are measured in kilowatts, while the associated costs are expressed in dollars. The table clearly shows that when the photovoltaic system is unable to operate, such as during nighttime, its power output becomes zero. Consequently, other units are necessary to meet the system load. The analyzed system exhibits two peak loads in a day. The first peak occurs during daytime office hours, while the second peak arises at night due to heating systems, as the investigation is conducted during the winter season. As shown in Figure (5), the cost of operating the MG from 12 am to 6 pm significantly decreases compared to the previous hour, despite the grid load being at its peak. This decrease in cost is attributed to the presence of the photovoltaic system in the MG, generating its maximum power output during this time period and helping to minimize operating costs. However, during the night peak when the photovoltaic system is inactive, the system's operational cost is higher than other hours. The absence of the photovoltaic system during this period increases reliance on other sources, resulting in higher costs. The following section explores the inclusion of storage units in the island mode to investigate the operation of the microgrid under these conditions.

Table.1.
DERs specifications used in MG under consideration

Power source	O&M Cost ($)	SU cost ($)	SD cost ($)	Fuel cost ($)	P_{min} (kW)	P_{max} (kW)
PV	0.639	0	0	0	0	50
Wind	0.778	0.342	0.186	0	0	85
FC	0.241	0.337	0.322	0.233	8	45
MT	0.103	0.281	0.186	0.178	8	45
Upstream network	-	-	-	-	-180	+180

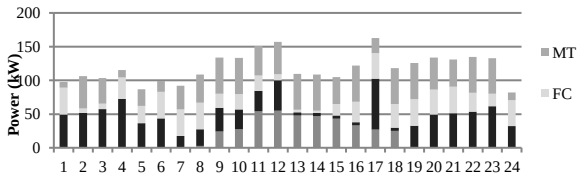

Fig. 4. Daily power generated by DERs in islanding mode without using ESS

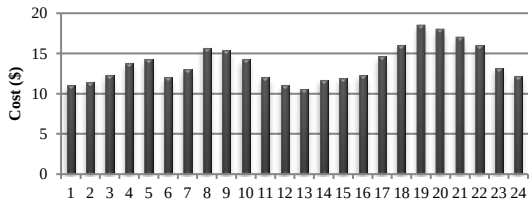

Fig. 5. Daily cost of islanding mode without using ESS

B) Islanding mode in the presence of ESS

In this particular scenario, the photovoltaic system operates at its maximum power output during the day, and any surplus power is stored in the battery. Later, during nighttime, the battery is utilized to supply power. The analysis involves determining the optimal battery capacity required for the MG system and then identifying the optimal production arrangement for the available resources within the MG. To incorporate the batteries into the optimization process, the proposed algorithm is employed, utilizing the technical information provided earlier about the batteries, as well as the various combinations illustrated in Figure (6), which represent a range of battery capacities and energy levels. The profitability observed in this scenario is attributed to the lower operational cost of the PV system compared to other DERs. Specifically, electricity is obtained from the PV system at a rate of 7.74 dollars/kWh, while it is supplied at a cost of 9.12 dollars/kWh during non-PV operating hours, as indicated in Figure (7). Since the MG operates in island mode without any connection to the upstream network, discussions about market prices are irrelevant. Furthermore, the total power output capacity achieved by the PV system is 309.48 kilowatts. Out of this capacity, 208.21 kilowatts are allocated through the unit arrangement process for production purposes, leaving only 101.49 kilowatts available for battery charging. Consequently, the evaluated optimum capacity for the CAES system is determined to be 48.31 kW, which can be practically utilized. After analyzing the MG in island mode, the focus now shifts to examining the network connection mode and its characteristics. In this scenario, the objective is to compare the cost of producing one kilowatt of power using the most expensive DG resource with the current electricity price in the market.

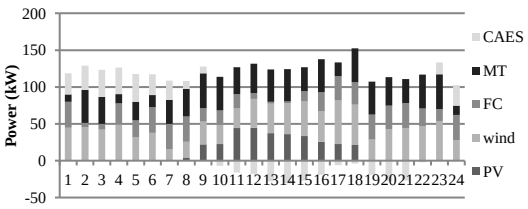

Fig. 6. Figure (6), Daily power generated by DERs in islanding mode using ESS

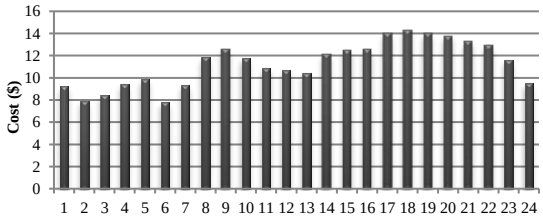

Fig. 7. Daily cost of islanding mode using ESS

If the market price is lower, it becomes advantageous to source power from the upstream network. Conversely, if the market price exceeds the cost of local power generation, it becomes desirable to supply power locally within the MG. By conducting this comparison, stakeholders can make informed decisions regarding the most cost-effective approach for power supply. If the market price is more favorable, accessing electricity from the upstream network proves beneficial as it allows the MG to utilize external resources at a lower cost. On the other hand, if the local power generation cost is lower than the market price, supplying power within the MG becomes a preferable option as it ensures greater control and self-sufficiency. This analysis of the network connection mode and its associated factors enables stakeholders to optimize their power procurement strategy, considering the prevailing market conditions and the cost-effectiveness of local power generation. By making the appropriate choice between accessing power from the upstream network and supplying power within the MG, stakeholders can maximize their financial benefits and ensure the efficient operation of the MG system.

C) Grid-connected mode without using ESS

The results regarding the unit production arrangement in the network connection mode, without storage, have been summarized in Figure (8). It is important to emphasize that these outcomes are presented from the perspective of the MG network. Therefore, a negative power exchange with the network signifies power received from the network, while a positive exchange indicates power injected into the network. According to Figure (8), it is evident that in only five time periods, sourcing electricity from the upstream network reduces the costs and profits of the MG. Therefore, the unit production arrangement during these four hours corresponds to the details provided in the aforementioned table. Additionally, the results indicate that engaging in power exchange with the upstream network can increase the MG's profitability. In this case, the profitability is 18.32% higher compared to the previous two scenarios, primarily due to the significant contribution of the upstream network in supplying power. Several factors contribute to this increased profitability:

- Cost Savings: By relying on the upstream network for a significant portion of the power supply, companies can reduce their own power generation costs. This includes expenses related to operating and maintaining power generation facilities, as well as the cost of fuel or energy sources. The savings achieved through this arrangement contribute to overall profitability.
- Scalability: Leveraging the upstream network allows for greater scalability and flexibility in meeting power demands. Companies can easily adjust their power consumption based on fluctuating needs without requiring substantial infrastructure investments. This agility enables efficient resource allocation and optimization, resulting in improved profitability.
- Risk Mitigation: Depending solely on internal power generation can be risky, as it exposes companies to potential disruptions or failures in their own power infrastructure. By diversifying their power sources and relying on the more reliable upstream network, businesses can mitigate these risks and ensure a consistent power supply. This stability translates into enhanced operational efficiency and ultimately higher profitability.
- Focus on Core Competencies: By relying on the upstream network, companies can allocate resources and expertise to their core competencies rather than power generation. This allows for more efficient resource allocation, increased productivity, and better financial outcomes.
- Environmental Considerations: In many cases, the upstream network may utilize renewable energy sources or cleaner technologies, resulting in a reduced carbon footprint. By aligning with sustainable practices and benefiting from associated incentives, businesses can enhance their corporate image, attract environmentally conscious customers, and potentially access additional revenue streams.

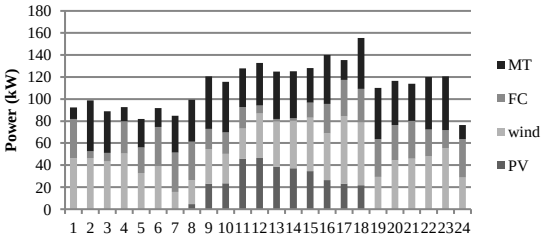

Fig. 8. Daily power generated by DERs in grid-connected mode without using ESS

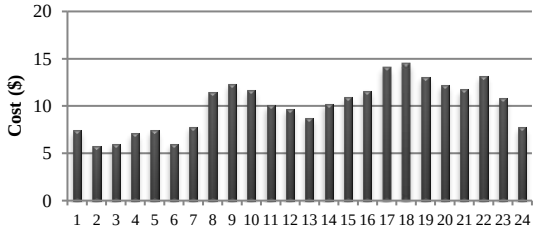

Fig. 9. Daily cost of grid-connected mode without using ESS

D) Grid-connected mode using ESS

This section is dedicated to determining the optimal storage capacity that maximizes the profitability of the microgrid when connected to the upstream network. It is assumed that the microgrid is already installed and equipped with distributed production resources. Additionally, the microgrid has the capability of exchanging 180 kilowatts of power with the upstream grid on a financial day. The proposed algorithm is once again employed to identify the optimal production arrangement and battery capacity. In this case, the battery functions by receiving and charging power from the upstream network during periods of low market prices and supplying power to the market during peak load periods when the market price is higher. After evaluating the overall situation of microgrid utilization and the availability of resources, it can be concluded that if the battery capacity is 28 kW or less, utilizing the entire capacity for storing energy from the upstream network during non-peak conditions and subsequently injecting it into the network during peak periods will yield the maximum achievable profit. This approach is advantageous because the electricity market price during peak periods significantly exceeds the operating cost of the microgrid units. However, it is important to note that out of the outlined scenarios, only 33.24 kilowatts of power exchange with the upstream network are possible during a financial day. Consequently, the scenario that generates the highest profit for the microgrid is selected. In this case, the most favorable scenario involves injecting 18.48 kW of power into the upstream network, resulting in a profit of $7.67 according to Figures (10) and (11).

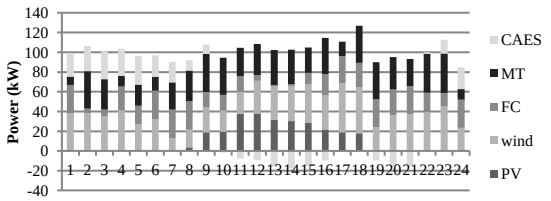

Fig. 10. Daily power generated by DERs in grid-connected mode using ESS

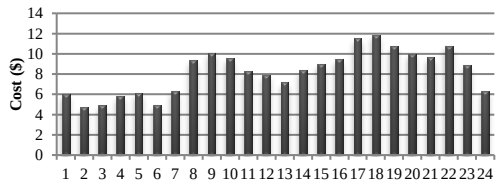

Fig. 11. Daily cost of grid-connected mode using ESS

The simulation results presented in this study offer valuable insights into the operation and optimization of a MG system that utilizes decentralized power generation resources like micro turbines and fuel cells. The analysis focuses on two primary modes of operation: islanding mode (without energy storage) and grid-connected mode (with energy storage). The discussion highlights the key findings and implications of each mode, taking into account system performance, financial management, and overall efficiency. In the islanding mode without energy storage, the MG operates independently without relying on the main grid. However, the absence of energy storage limits the system's ability to effectively manage fluctuations in energy generation and demand. The simulation results demonstrate that the presence of a photovoltaic system significantly reduces operating costs during the day when it generates maximum power output. However, operational costs increase during nighttime hours when the PV system is inactive, emphasizing the need for energy storage to improve flexibility and resilience. Energy storage allows for the storage of excess energy during low-demand periods and its release during peak demand periods, leading to cost savings and improved overall performance.

The analysis also considers the network connection mode, where the MG can procure power from the upstream grid or supply power locally within the MG. By comparing the cost of producing one kilowatt of power using the most expensive distributed generation resource with the prevailing market price, stakeholders can make informed decisions about the most cost-effective approach. If the market price is lower than the cost of local power generation, accessing electricity from the upstream network becomes advantageous. Conversely, if the local power generation cost is lower than the market price, supplying power within the MG becomes preferable. This analysis enables stakeholders to optimize their power procurement strategy based on market conditions and cost-effectiveness, maximizing financial benefits and ensuring efficient operation of the MG system. In the grid-connected mode with energy storage, the simulation results focus on determining the optimal storage capacity to maximize the MG's profitability when connected to the upstream network. The battery operates by receiving and charging power from the upstream network during periods of low market prices and supplying power to the market during peak load periods when the market price is higher. The results indicate that profitability is influenced by the relationship between the battery capacity and market conditions. The optimal approach involves storing energy from the upstream network during non-peak conditions and injecting it into the network during peak periods, where the market price significantly exceeds the MG's operating costs. This strategy allows for significant profit generation and highlights the importance of optimizing storage capacity based on market dynamics.

5. Discussion

The simulation results emphasize the broader implications of the findings. In the grid-connected mode without energy storage, leveraging the upstream network for a significant portion of the power supply enables cost savings, scalability, risk mitigation, focus on core competencies, and environmental considerations. By relying on the more reliable upstream network, businesses can enhance operational efficiency, reduce their carbon footprint, and potentially access additional revenue streams. In the grid-connected mode with energy storage, the optimal utilization of storage capacity allows for maximum profit generation by aligning energy supply with market conditions.

To conclude the paper, there are several scenarios for reliability evaluation (RE) that investigate the influence of CAESs on the operation mechanism of the microgrid.

A) Scenario 1: Basic RE

In this scenario, a basic RE of the energy storage system in the MG is considered. The provided data includes λ and MTTR for the battery, converter, and control system. The system availability is calculated based on the MTBF and MTTR of the system components. The $MTBF_{sys}$ is obtained by taking the inverse of the sum of the component λ. The MTTR_sys is calculated by summing the individual component MTTRs. The reliability (R) is calculated as the probability that the system operates without failure for a given period. It is derived from the system availability (A) using the formula discussed in [32-35]. The maintainability (M) represents the ability to repair and restore the system to an operational state within a given time. It is calculated as the ratio of $MTBF_{sys}$ to $MTBF_{sys}$ plus twice the $MTTR_{sys}$. Table (2) presents the main parameters used for the RE of the CAES in the MG, while Table (3) illustrates the results of this scenario. It shows that using CAES will increase the system

reliability, availability and maintainability. In addition, the simulation results show that the MG power system can continue its normal operation for many hours without any interruption or loss of load and energy not served. Scenario 2: Redundancy Analysis

In this second scenario, the impact of redundancy on the reliability of the energy storage system is analyzed. The data provided includes the same λ and MTTR for the components as in Scenario 1, along with the number of redundant batteries (N_{red}). Considering the N_{red} redundant batteries in parallel, the system reliability is calculated using the k-out-of-n method. Table (4) presents the main parameters used for this scenario. This method evaluates the system reliability based on the number of redundant components needed for the system to operate successfully. The reliability of a single battery ($R_{battery}$) is raised to the power of the number of redundant batteries (k), multiplied by the complement of $R_{battery}$ raised to the power of the difference between N_{red} and k. By adding redundancy to the system, the overall reliability and availability are expected to improve, as the failure of a single component does not result in a complete system failure as the results are shown in Table (5).

B) Scenario 3: Failure Modes and Effects Analysis

In this scenario, a failure modes and effects analysis (FMEA) for the energy storage system is performed. Along with the λ and MTTRs for the components, data is provided for two specific failure modes: overheating of the converter ($FM1$) and communication failure in the control system ($FM2$). For each failure mode, we consider the probability of occurrence (P_{FM}) and the consequence (C_{FM}). The overall system reliability is calculated by incorporating the probabilities and consequences of different failure modes using fault tree analysis. Considering the data represented in Table (6), the system availability, MTBF, MTTR, and reliability indices are calculated based on the same formulas and principles as in Scenario 1, considering the probabilities and consequences of FM1 and FM2 as shown in Table (7). By conducting a failure modes and effects analysis, we can identify and prioritize critical failure modes, understand their impact on system reliability, and develop appropriate mitigation strategies to enhance the overall reliability of the energy storage system.

Table.2.
Table 2, main parameters of scenario 1 used for the RE of CAES in the MG

Parameter	***Value***
Battery failure rate	0.001 failures/hour
Converter failure rate	0.0005 failures/hour
Control system failure rate	0.0002 failures/hour
MTTR for battery	3 hours
MTTR for converter	4 hours
MTTR for control system	2 hours

Table.3.
Table 3, the results of basic RE analysis

Metric	***Value***
System Availability	0.9982
MTBF for battery	1000 hours
MTBF for converter	2000 hours
MTBF for control system	5000 hours
MTTR for system	9 hours
Reliability (R)	0.999991
Availability (A)	0.9982
Maintainability (M)	0.9991

Table.4.
Main parameters of scenario 2 named redundancy analysis

Parameter	***Value***
Battery failure rate	0.001 failures/hour
Converter failure rate	0.0005 failures/hour
Control system failure rate	0.0002 failures/hour
MTTR for battery	3 hours
MTTR for converter	4 hours
MTTR for control system	2 hours
Number of redundant batteries	2

Table.5.
The results of redundancy analysis scenario

Metric	***Value***
System Availability	0.9994
MTBF for battery	1000 hours
MTBF for converter	2000 hours
MTBF for control system	5000 hours
MTTR for system	9 hours
Reliability (R)	0.999995
Availability (A)	0.9994
Maintainability (M)	0.9996

Table.6.
Main parameters of scenario 3 named FMEA

Parameter	*Value*
Battery failure rate	0.001 failures/hour
Converter failure rate	0.0005 failures/hour
Control system failure rate	0.0002 failures/hour
MTTR for battery	3 hours
MTTR for converter	4 hours
MTTR for control system	2 hours
Probability of FM1 ($\boldsymbol{P_{FM1}}$)	0.0003
Consequence of FM1 ($\boldsymbol{C_{FM1}}$)	$5000
Probability of FM2 ($\boldsymbol{P_{FM2}}$)	0.0002
Consequence of FM2 ($\boldsymbol{C_{FM2}}$)	$3000

Table.7.
The results of FMEA scenario

Metric	*Value*
System Availability	0.9982
MTBF for battery	1000 hours
MTBF for converter	2000 hours
MTBF for control system	5000 hours
MTTR for system	9 hours
Reliability (R)	0.999991
Availability (A)	0.9982
Maintainability (M)	0.9991

6. Conclusion

The optimization of microgrid planning was addressed in this study by considering the integration of CAES systems. A novel approach, the HANN-MDA, was proposed to determine the optimum CAES capacity in microgrid designs. The HANN-MDA method combined the learning capabilities of artificial neural networks with the optimization power of the modified dragonfly algorithm, enabling an efficient and accurate determination of the optimal CAES capacity. The effectiveness of the HANN-MDA method in achieving cost savings and improving microgrid performance was demonstrated through simulation results. By considering the integration of renewable energy sources and the storage capabilities of CAES, the proposed method effectively minimized the overall cost of microgrid operation and facilitated the optimal utilization of renewable energy resources, enhancing the grid's resilience and sustainability. The findings highlight the importance of considering CAES in microgrid planning and emphasize the valuable tool that the HANN-MDA method provides for designing and operating cost-effective and sustainable microgrid systems. Further studies can explore the applicability of the HANN-MDA method in different microgrid scenarios, taking into account additional factors such as environmental impacts and grid resiliency requirements.

Nomenclature

Sets	
T	Time periods
W	Wind turbines
S	Solar PV
M	Microturbines
G	Generators (W, S, M)
L	Set of loads
P	Pollutants (CO_2, SO_2, NO_x)
Parameters	
$D(t)$	Electric load at time (t) (MW)
C_w, C_s, C_m	Generator costs $(\$/MWh)$
$P_{w\max}(t), P_{s\max}(t)$	Max renewable power (MW)
$P_{m\min}, P_{m\max}$	Microturbine limits (MW)
C_{ens}	Cost of energy not served (MWh)
C_{ex}	Cost of excess generation (MWh)
$E_g(p)$	Emission rate of pollutant (p) (kg/MWh)
$CP(p)$	Penalty for pollutant (p) (kg)
eff_c	CAES compression efficiency
eff_d	CAES discharge efficiency
E_{caesmax}	Max CAES energy (MWh)
R	Gas constant (J/kgK)
T_0	Temperature (K)
P_0	Pressure (Pa)
cp	Specific heat (J/kgK)
$n_{\min}, n_{\max}$	Polytropic index limits
$QLHV$	Lower heating value (MJ/kg)
Ca	Cost of air (kg)
M_{emission}	Maximum allowable emissions cost (MWh)
$U_w(t), U_s(t)$	Uncertainty factors for wind and solar power
x_{tl}^{DR}	Binary variable indicating whether demand response is activated for load l during period (t)
Decision Variables	
$P_g(t)$	Power output of generator (g) at time (t) (MW)
$P_l(t)$	Power demand for for load l during period (t)
$P_{\text{caes\_c}}(t)$	CAES compression power at time (t) (MW)
$P_{\text{caes\_d}}(t)$	CAES discharge power at time (t) (MW)
$E_{\text{caes}}(t)$	CAES energy level at time (t) (MWh)
$P_{\text{ens}}(t)$	Power not served at time (t) (MW)
$P_{\text{ex}}(t)$	Excess power at time (t) (MW)

$E_p(t)$	Emissions of pollutant (p) at time (t) (kg)
$U_w(t)$	Uncertainty factor for wind power at time (t)
$U_s(t)$	Uncertainty factor for solar power at time (t)

References

[1] Shafiee, M., Jazebi, S., Zamani, A. A., & Karimzadeh, F. (2023). Power Management and Dynamic Assessment of a Hybrid Wind, PV, and Battery Energy System. International Journal of Smart Electrical Engineering, 12(03), 165-171.

[2] Salehi, M. H., Moradian, M., Moazzami, M., & Shahgholian, G. (2022). Distributed Energy Technologies Planning and Sizing in a Sample Virtual Power Plant Using Speedy Particle Swarm Optimization Algorithm. International Journal of Smart Electrical Engineering.

[3] Alayi, R., Ebazadeh, Y., & Jahangiri, M. (2023). Modeling and Optimization Combined Heat and Power with photovoltaic/Thermal system. International Journal of Smart Electrical Engineering.

[4] Mortazi, A., Saeed, S., & Akbari, H. (2023). Optimizing Operation Scheduling in a MG Considering Probabilistic Uncertainty and Demand Response Using Social Spider Algorithm. International Journal of Smart Electrical Engineering, 12(02), 113-125.

[5] Al-Dhaifallah, M., Alaas, Z., Rezvani, A., Le, B. N., & Samad, S. (2023). Optimal day-ahead economic/emission scheduling of renewable energy resources based MG considering demand side management. Journal of Building Engineering, 76, 107070.

[6] Rahmani, E., Mohammadi, S., Zadehbagheri, M., & Kiani, M. (2023). Probabilistic reliability management of energy storage systems in connected/islanding MGs with renewable energy. Electric Power Systems Research, 214, 108891.

[7] Rabi, A. M., Radulovic, J., & Buick, J. M. (2023). Comprehensive review of compressed air energy storage (CAES) technologies. Thermo, 3(1), 104-126.

[8] Bin, L., Shahzad, M., Javed, H., Muqeet, H. A., Akhter, M. N., Liaqat, R., & Hussain, M. M. (2022). Scheduling and Sizing of Campus MG Considering Demand Response and Economic Analysis. Sensors, 22(16), 6150.

[9] Rezaeeian, S., Bayat, N., Rabiee, A., Nikkhah, S., & Soroudi, A. (2022). Optimal Scheduling of Reconfigurable MGs in Both Grid-Connected and Isolated Modes Considering the Uncertainty of DERs. Energies, 15(15), 5369.

[10] Emam, A. A., Keshta, H. E., Mosa, M. A., & Ali, A. A. (2023). Bi-level energy management system for optimal real time operation of grid tied multi-nanogrids. Electric Power Systems Research, 214, 108957.

[11] Huang, C., Zong, Y., You, S., Træholt, C., Zheng, Y., Wang, J., ... & Xiao, X. (2023). Economic and resilient operation of hydrogen-based MGs: An improved MPC-based optimal scheduling scheme considering security constraints of hydrogen facilities. Applied Energy, 335, 120762.

[12] Zheng, C., Eskandari, M., Li, M., & Sun, Z. (2022). GA−Reinforced Deep Neural Network for Net Electric Load Forecasting in MGs with Renewable Energy Resources for Scheduling Battery Energy Storage Systems. Algorithms, 15(10), 338.

[13] Fei, L., Shahzad, M., Abbas, F., Muqeet, H. A., Hussain, M. M., & Bin, L. (2022). Optimal energy management system of IoT-enabled large building considering electric vehicle scheduling, distributed resources, and demand response schemes. Sensors, 22(19), 7448.

[14] Zhu, Y., Li, G., Guo, Y., Li, D., & Bohlooli, N. (2023). Modeling Optimal Energy Exchange Operation of MGs Considering Renewable Energy Resources, Risk-based Strategies, and Reliability Aspect Using Multi-objective Adolescent Identity Search Algorithm. Sustainable Cities and Society, 91, 104380.

[15] Mansouri, S. A., Nematbakhsh, E., Ahmarinejad, A., Jordehi, A. R., Javadi, M. S., & Marzband, M. (2022). A hierarchical scheduling framework for resilience enhancement of decentralized renewable-based MGs considering proactive actions and mobile units. Renewable and Sustainable Energy Reviews, 168, 112854.

[16] Michael, N. E., Hasan, S., Al-Durra, A., & Mishra, M. (2023). Economic scheduling of virtual power plant in day-ahead and real-time markets considering uncertainties in electrical parameters. Energy Reports, 9, 3837-3850.

[17] Armioun, M., Nazar, M. S., Shafie-khah, M., & Siano, P. (2023). Optimal scheduling of CCHP-based resilient energy distribution system considering active MGs' multi-carrier energy transactions. Applied Energy, 350, 121719.

[18] Tostado-Véliz, M., Ghadimi, A. A., Miveh, M. R., Sánchez-Lozano, D., Escamez, A., & Jurado, F. (2022). A Novel Stochastic Mixed-Integer-Linear-Logical Programming Model for Optimal Coordination of Hybrid Storage Systems in Isolated MGs Considering Demand Response. Batteries, 8(11), 198.

[19] Basak, S., & Bhattacharyya, B. (2023). Optimal scheduling in demand-side management based grid-connected MG system by hybrid optimization approach considering diverse wind profiles. ISA transactions.

[20] Bolurian, A., Akbari, H., & Mousavi, S. (2022). Day-ahead optimal scheduling of MG with considering demand side management under uncertainty. Electric Power Systems Research, 209, 107965.

[21] Sharma, P., Mathur, H. D., Mishra, P., & Bansal, R. C. (2022). A critical and comparative review of energy management strategies for MGs. Applied Energy, 327, 120028.

[22] Aboutalebi, M., Nazar, M. S., Shafie-khah, M., & Catalão, J. P. (2022). Optimal scheduling of self-healing distribution systems considering distributed energy resource capacity withholding strategies. International Journal of Electrical Power & Energy Systems, 136, 107662.

[23] Lamari, M., Amrane, Y., Boudour, M., & Boussahoua, B. (2022). Multi-objective economic/emission optimal energy management system for scheduling micro-grid integrated virtual power plant. Energy Science & Engineering, 10(8), 3057-3074.

[24] Dey, B., Basak, S., & Pal, A. (2022). Demand-side management based optimal scheduling of distributed generators for clean and economic operation of a MG system. International Journal of Energy Research, 46(7), 8817-8837.

[25] Eskandari, M., Rajabi, A., Savkin, A. V., Moradi, M. H., & Dong, Z. Y. (2022). Battery energy storage systems (BESSs) and the economy-dynamics of MGs: Review, analysis, and classification for standardization of BESSs applications. Journal of Energy Storage, 55, 105627.

[26] Albaker, A. (2023). Reliability-Constrained Optimal Scheduling of Interconnected MGs. Engineering, Technology & Applied Science Research, 13(3), 11042-11050.

[27] Kabiri-Renani, Y., Daneshvar, M., & Mohammadi-Ivatloo, B. (2022). Transactive energy revolution: Innovative leverage for reliable operation of modern energy networks—A critical review. IET Renewable Power Generation, 16(15), 3368-3383.

[28] Gülcü, Ş. (2022). Training of the feed forward artificial neural networks using dragonfly algorithm. Applied Soft Computing, 124, 109023.

[29] Abdulameer, A. T. (2018). An improvement of MRI brain images classification using dragonfly algorithm as trainer of

artificial neural network. Ibn AL-Haitham Journal for Pure and Applied Science, 31(1), 268-276.

[30] Ali, G. A., Abubakar, H., Alzaeemi, S. A. S., Almawgani, A. H., Sulaiman, A., & Tay, K. G. (2023). Artificial dragonfly algorithm in the Hopfield neural network for optimal Exact Boolean k satisfiability representation. Plos one, 18(9), e0286874.